Experimental Thermal and Fluid Science 44 (2013) 875–882

Contents lists available at SciVerse ScienceDirect

Experimental Thermal and Fluid Science

journal homepage: www.elsevier.com/locate/etfs

Effect of inventory on the heat performance of copper–water loop heat pipe

Li Zhang, Jiayin Xu, Hong Xu *

State-Key Laboratory of Chemical Engineering, School of Mechanical and Power Engineering, East China University of Science and Technology, Shanghai 200237, China

ARTICLE INFO

Article history:
Received 27 July 2012
Received in revised form 29 September 2012
Accepted 29 September 2012
Available online 13 October 2012

Keywords:
Loop heat pipe
Copper wick
Start-up
Inventory
Heat-transfer capacity

ABSTRACT

The operating characteristics of a copper–water loop heat pipe (LHP), including start-up property, heat-transfer capacity, and heat resistance, under four different charge ratios (52.2–78.3%) were experimentally investigated. The LHP had a cylindrical evaporator (22 mm diameter and 80 mm long) with a sintered copper wick, and the clearance between the evaporator envelope and the wick surface was eliminated to attain a low heat contact resistance. The porosity of the wick was 44.54%, and the effective pore radius was 19.11 μm. The experiment showed that higher inventory is an effective method in keeping the wick saturated within the low heat-load range and in supplying adequate flow of the subcooled liquid from the condenser to cool the water in the compensation chamber within the medium heat-load range. Thus, fast start-up of 260 s (heat load: 30 W; heat flux: 8.5×10^3 W/m^2), maximum heat-transfer capacity of 500 W (under allowable evaporator wall temperature of 85 °C), and minimum LHP thermal resistance of 0.075 °C/W (under 500 W heat load) were realized by the LHP charged with an optimal 69.6% volume ratio.

1. Introduction

Loop heat pipe (LHP) is an effective two-phase heat-transfer device invented by Russian scientist Maydanik [1] in 1972. LHP has become one of the most promising candidates in dissipating high heat load from confined spaces and controlling the wall temperature of electronic components because of its number of advantages in terms of robust operation, flexible heat-transport lines, and operability against gravity [2]. As no power is input to the working fluid circulation in the LHP, creating a pressure drop to start the circulation of the working fluid from a stationary state requires a certain period of time, which is considered as the start-up time. If the start-up time is long, the wall temperature will exceed the allowable temperature, resulting in damage of the electronic components. Hence, to prevent damage to the electronic components, a good LHP must be characterized by fast start-up and high heat-transfer capacity.

In the past, the copper–water LHP was considered as unsuitable for operation at temperatures below 100 °C due to massive heat leak resulting from high thermal conductivity of copper, as well as low derivative dP/dT value of water below 100 °C [3]. Heat leak is defined as that part of the heat applied to the evaporator transfers to the compensation chamber and makes the liquid temperature in the compensation chamber increase because of the thermal conduction in the capillary wick and metallic evaporator envelope, as well as the vapor leakage [4]. As a result of the heat leak, it is difficult to establish an adequate temperature difference (ΔT_w) and pressure difference (ΔP_{ext}) for start-up and operation. According to the second condition of LHP serviceability [1], ΔT_w is the temperature difference between the evaporating surface of the wick and the temperature of the compensation chamber, and ΔP_{ext} is the pressure difference to drive the working fluid through liquid line to the compensation chamber. In addition, high liquid temperature in the compensation chamber resulting from heat leak will increase the LHP saturation temperature. Thus, the amount of heat leak is considered as the main factor that determines the heat performance of LHPs. If heat leak is successfully minimized, adequate temperature difference (ΔT_w) and low compensation chamber temperature would be realized, which could result in fast start-up, low saturation temperature, and high heat-transfer capacity during LHP operation.

To effectively suppress heat leak, plastic [5,6] and ceramic [7,8] wicks have been extensively used in the evaporator. These wicks present very low thermal conductivity, desirable in the alleviation of heat leak. However, the permeability (the rate of flow of a liquid or gas through a porous media) of these types of wicks is around 10^{-14} m^2, it is very low and results in increase in the pressure drop through the capillary wick, dry zone in the wick, and low heat-transfer capacity [7,8]. In contrast, wicks made of sintered metal particles can obtain large permeability in the range of 10^{-11}–10^{-13} m^2, which can prevent dry zone in the wick that results from low permeability. Thus, sintered metal wicks made of nickel [9,10] are widely used because of easy access and compatibility with most working fluids. Additionally, other wicks made of low thermal conductivity materials, such as stainless steel [11,12], titanium

* Corresponding author. Tel.: +86 021 64252847; fax: +86 021 64253810.
E-mail address: hxu@ecust.edu.cn (H. Xu).

0894-1777/$ - see front matter © 2012 Elsevier Inc. All rights reserved.
http://dx.doi.org/10.1016/j.expthermflusci.2012.09.030

Nomenclature

ΔP_{ext}	pressure difference between the evaporator and the compensation chamber
Q	heat input
R_{cont}	contact thermal resistance
R_{dry}	dry zone thermal resistance
R_e	evaporator thermal resistance
R_w	wick thermal resistance
R_{wall}	evaporator wall thermal resistance
R_{LHP}	LHP thermal resistance
T_{cc}	compensation chamber temperature
T_{ci}	condenser inlet temperature
T_{co}	condenser outlet temperature
T_{cond}	condenser temperature
T_{ew}	evaporator wall temperature
T_v	vapor temperature
ΔT_w	temperature difference between two sides of the wick
T_{we}	external side of the wick temperature
T_{wi}	internal side of the wick temperature

[13], and nickel–copper alloys [14], have also been employed to fabricate capillary wicks. Compared with the copper wick, the above-mentioned wicks are suitable in suppressing heat leak. However, Singh et al. [15] pointed out that a compromise between lesser heat leak using a wick made from a low thermal conductivity material and efficient heat exchange using a wick with good thermal conductivity in the evaporation zone can be established. During operation, a copper wick has higher heat-transfer coefficient and lower thermal resistance than a nickel wick. Thus, the saturation temperature of LHP with a copper wick is lower than that with a nickel wick under medium heat-load range. Copper has been suggested as a better choice for heat exchange in the evaporation zone of LHP provided that the heat leak due to the use of copper can be efficiently minimized.

Recently, Maydanik et al. [3] has pointed out that the copper–water LHP with some improvements such as increases in the vapor line diameter and in the wick thickness is suitable for operation below 100 °C. In this manner, the required pressure difference (ΔP_{ext}) is reduced because of low friction-pressure losses in the large vapor line, and a sufficient temperature difference (ΔT_w) between thick wicks is easily formed. In addition, low vapor pressure below 100 °C allows the construction of evaporators with thin walls, leading to a low thermal resistance. These improvements result in maximum heat load of up to 1,200 W with a smooth start-up when the wall temperature is kept below 100 °C. A similar experiment using different copper wick thicknesses was also performed by Wang et al. [16], which showed that start-up time improved with increasing thickness because heat leak was reduced, and the temperature difference (ΔT_w) between the two sides of the wick increased. Suggestion was put forward that heat leak in a copper–water LHP can be suppressed using correct approaches, such as proper wick thickness and large vapor-line diameter, which could realize exceptionally high thermal characteristics.

Many literatures have focused on the effect of charge ratio on the operation mode of LHP. Boo et al. [17] have studied the effect of the fill charge on the thermal resistance and found a maximum heat load for an optimum value of the charge ratio from 40% to 50%. Joung et al. [11] have investigated the influence of the fluid inventory on the operating temperature of the LHP with a stainless steel wick, and found that the heat leak of lower fluid inventory is greater than that at higher fluid inventories. The experiment has shown that a minimum thermal resistance of 1.27 °C/W and a maximum heat load of 78 W are reached with a fluid inventory of 60.05%. Celata et al. [12] have conducted a series of tests to obtain the optimum fluid inventory of the LHP with a stainless steel wick, and found that a charge ratio from 60% to 80% is acceptable for the reliable start-up and steady-state operation of the LHP. Due to different sizes of the parts of the LHP, the results of the optimum charge ratio are of difference. Thus, it is necessary to find out the cause of this discrepancy. Besides that, the effect of fluid inventory on heat leak in improving the heat-transfer performance of copper–water LHPs operating below 100 °C has not been investigated until now.

In this paper, a copper–water LHP with a cylindrical evaporator was manufactured, and different water charge ratios (52.2–78.3%) were used to study its effect on heat leak. In addition, the LHPs, whose connection design that eliminates the clearance between the evaporator envelope and the wick surface has been proposed recently by Xu et al. [18], were tested. Thus, high thermal characteristic, minimum contact thermal resistance, and elimination of vapor leak were attained to promote heat-transfer efficiency in the LHP evaporation zone. Vapor leakage is regarded as another kind of heat leak because the vapor driven by pressure drop through the clearance leaks from the evaporation zone to the compensation chamber, which becomes more pronounced with the increase in heat load. To prevent vapor leakage, ceramic wicks fabricated using a high-precision machining process [7] were used, and EPDM (Ethylene propylene diene monomer) sealing around the wick [4] was performed.

2. Experimental apparatus and procedures

2.1. Experimental setup

Fig. 1a shows the schematic and the view of the closed LHP consisting of a cylindrical evaporator with a sintering capillary wick, a condenser, a compensation chamber, and two transport lines for the liquid and vapor flow. The tested LHP is shown in Fig. 1b The evaporator used in this study is made of brass (outer diameter 22 mm, 80 mm long). The vapor removal grooves are milled on the internal side of the evaporator envelope, as shown in Fig. 1c. In order to improve the heat-transfer properties of the LHP, the clearance

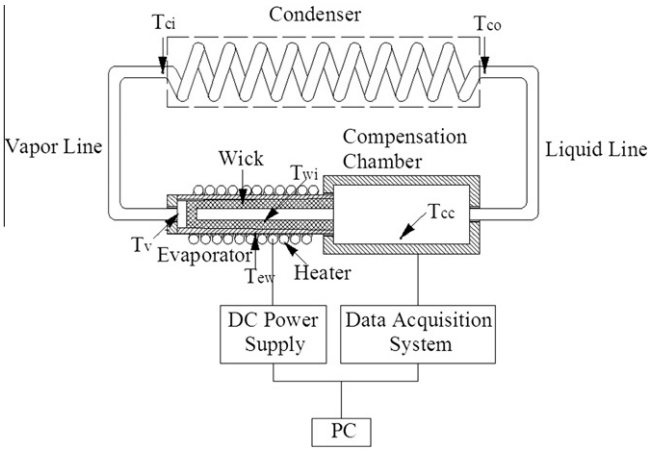

Fig. 1a. Schematic of the test set-up.

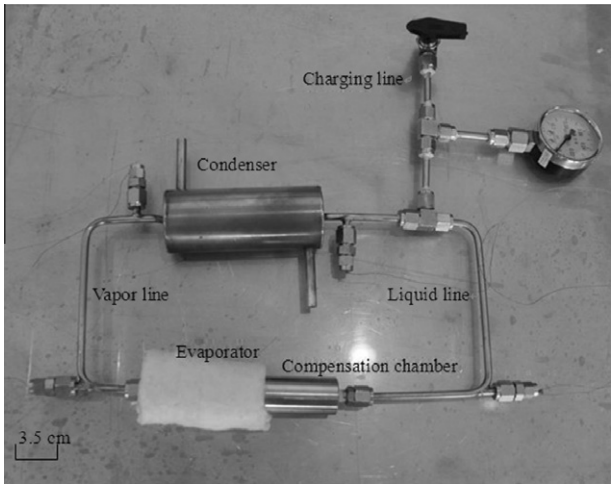

Fig. 1b. General view of LHP with cylindrical evaporator.

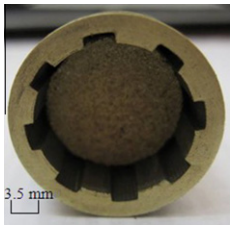

Fig. 1c. Cross section of the evaporator and the vapor removal groove.

Fig. 1d. The copper wick with the slope of 1°.

between the evaporator envelope and the copper wick surface is eliminated, and metallurgical bonding is created to minimize contact heat resistance and avoid vapor leak. The detailed manufacturing process of the evaporator is described in Xu et al. [18].

As shown in Fig. 1d, the conical copper wick is sintered by the particles with an average 139 μm diameter, which is 5 mm in radical thickness, 75 mm in length. The effective pore radius, the porosity and the permeability are 19.11 μm, 44.54% and 8.31×10^{-11} m^2, which are measured and calculated by the mercury porosimeter (PoreMaster-60 GT).

Except the evaporator envelop and the capillary wick, the other parts of the LHP are all made of stainless steel. A shell-tube heat exchanger is used as the condenser. It is a counter-flow condenser, and the water flow rate has been adjusted to 500 mL/min at 10 ± 0.5 °C, at the same time the ambient temperature is 12 ± 0.5 °C. The compensation chamber is used to accommodate excess water and bolted together with the evaporator. The vapor line is 300 mm in length, 4 mm in internal diameter. The liquid line with the length of 700 mm and internal diameter of 4 mm is used. The total volume of the LHP is 46.0 ml, and the combined volume of the evaporator and the compensation chamber is 23.2 ml. Hence, the volume ratio of the evaporator and the compensation chamber combined to the LHP is larger than 50%. The fluid inventory of the LHP must satisfy the equations for the cold and the hot cases which can be found in [19]. In the present LHP, the proper inventory is 26.8–37.7 ml between the cold and the hot cases.

Six *T*-type thermocouples are used for temperature measurement with an accuracy of ±0.5 °C. A sheathed thermocouple (1 mm sheath diameter, Omega Engineering, Inc.) is equipped to measure the wall temperature of the evaporator (T_{ew}). It is also used to identify the magnitude of the maximum heat transfer capacity when T_{ew} reaches around 85 °C. The other thermocouples (0.38 mm in diameter, Omega Engineering, Inc.) are inserted into the LHP to directly measure the fluid temperatures such as the evaporator outlet temperature (T_v, also vapor temperature), the inlet (T_{ci}) and outlet (T_{co}) temperatures of the condenser, the fluid temperature in the compensation chamber (T_{cc}) and the evaporator core temperature (T_{wi}, the thermocouple attaching to the internal surface of the wick). With internal temperature measurement, temperature readings are obtained and recorded at a frequency of 0.5 Hz by Agilent 34970A Data Logger/switch Unit.

Nickel-chrome wire (0.6 mm diameter) is used to serve as the simulation heater with external ceramic insulation layer. To minimize the heat exchange with the ambient, the evaporator is thermally insulated by a glass fiber layer. The heating power is adjusted by a DC power supply (Agilent N5769A) with maximum capacity of 100 V and 15 A, and the heat input area is 35.23 cm^2 (22 mm evaporator diameter, 51 mm heat source length).

2.2. Testing procedures

Before the experiment, it is necessary to prove that the influence of air infiltration occurred in the present LHP can be neglected. The LHP is evacuated to a pressure of 6.0×10^{-5} Pa using a vacuum pump and a turbomolecular pump. After 24 h, the change of the absolute pressure was only 2.5×10^{-5} Pa, while the test run is always finished within 6 h. Hence, air infiltration into the LHP is negligible. After the pressure check, a selected volume of deionized water is charged into the LHP by using a graduated cylinder, which is degassed and preserved under vacuum prior to charging. According to proper inventory, they are from 26.8 ml (58.3%) to 37.7 ml (80.6%). The selected fluid inventories are 24 ml, 28 ml, 32 ml and 36 ml, which corresponds to the charge ratios of 52.2%, 60.9%, 69.6% and 78.3%. The experiment is started with the charge ratio of 52.2% (24 ml) when the evaporator and the compensation chamber (23.2 ml) are just full of liquid. The ending 78.3% (36 ml) is very close to the limit inventory of 80.6% (37.7 ml).

The start-up parameters such as the superheat, the start-up time and the temperature profiles are obtained during the start-up process of the LHP. In the present study, positive elevation, namely the condenser being located above the evaporator, is selected. As a result of that, both the vapor grooves and the evaporator core are flooded with the working liquid. During the start-up process, a constant heat load of 30 ± 1 W is imposed to the evaporator. A successful start can be recognized from the temperature readings of the six thermocouples monitoring the fluid movement and temperature distribution in the LHP.

Once the LHP gets start, the heat-transfer capacity test begins at a heat load of 50 W with a stepwise increment of 50 W. For each heat load, a steady state, namely the evaporator wall temperature and the vapor temperature are kept within a maximum limit of ±0.5 °C, should be accomplished. After that, the temperature readings of thermocouples are recorded and averaged. When the evaporator wall temperature reaches around 85 °C, the test will be stopped. At the same time, the heat load applied to the LHP is considered as the heat transfer capacity.

2.3. Data reduction

During the start-up process, the second condition of LHP serviceability [1] is the necessity of creating a sufficient temperature

(ΔT_w) and pressure (ΔP_{ext}) differences across the wick, which is defined as:

$$\left.\frac{dP}{dT}\right|_{\bar{T}}(\Delta T_w) = \Delta P_{ext} \quad (1)$$

where ΔT_w is the temperature difference between the evaporating surface of the wick (T_{we}) and the saturation temperature of the compensation chamber. Since T_{we} can be considered as the vapor temperature T_v and the saturation temperature of the compensation chamber is close to T_{cc}, temperature difference between T_v and T_{cc} is approximately considered as the value of ΔT_w in the discussion. dP/dT is the derivative obtained by the slope of the saturation line at the temperature of the compensation chamber.

To get an enough pressure difference (ΔP_{ext}) for the working fluid circulation, either a large enough temperature difference (ΔT_w) or a high value of dP/dT is required. In other words, heat leak should be alleviated to get an enough temperature difference (ΔT_w), otherwise that will result in a high value of dP/dT with a high saturation temperature of the compensation chamber.

Furthermore, the thermal resistance is one of the most important parameters that reflect the performances of the LHP during the heat transfer capacity tests. The evaporator thermal resistance was defined as:

$$R_e = (T_{ew} - T_v)/Q \quad (2)$$

where T_{ew} is the evaporator wall temperature; T_v is the vapor temperature; Q is the input power.

And the LHP thermal resistance was defined as:

$$R_{LHP} = (T_{ew} - T_{cond})/Q = \left(T_{ew} - \frac{(T_{ci} + T_{co})}{2}\right)\Big/Q \quad (3)$$

where T_{ew} is the evaporator wall temperature; T_{cond} is the condenser temperature (calculated by averaging the readings from the condenser inlet and outlet temperature, T_{ci} and T_{co}).

An uncertainty analysis has been performed according to the method proposed by Kline and McClintock [20]. The estimated uncertainties of diameter, length and area are ±0.23%, ±0.10% and ±0.25%, respectively. The uncertainty of temperature is ±0.5 K for the thermocouples. The maximum value of uncertainties of electric current, voltage, input power, heat flux, evaporator thermal resistance and LHP thermal resistance are ±0.37%, ±0.40%, ±0.52%, ±0.59%, ±3.74% and ±4.01%, respectively.

3. Results and discussion

3.1. LHP start-up process

The LHP tests were conducted using identical copper wicks under water charge ratios of 52.2%, 60.9%, 69.6%, and 78.3%. Before the tests, the LHP was set in a positive elevation, i.e., the evaporator was located below the condenser. As mentioned earlier, the evaporator and compensation chamber combined volume ratio was approximately 50%. Under these inventories, both the vapor grooves and the wick were saturated with water, and no vapor–liquid interface existed in the evaporation zone. A constant heat load of 30±1 W was applied to the evaporator during the start-up process, which approximately corresponded to a heat flux of 8.5×10^3 W/m^2. Maydanik et al. [3] opined that 8.5×10^3 W/m^2 heat flux can be considered a low heat flux (i.e., the value does not exceed 5.0×10^4 W/m^2).

Fig. 2 shows the LHP start-up processes under different charge ratios, and Fig. 3 shows the temperature differences (ΔT_w) during

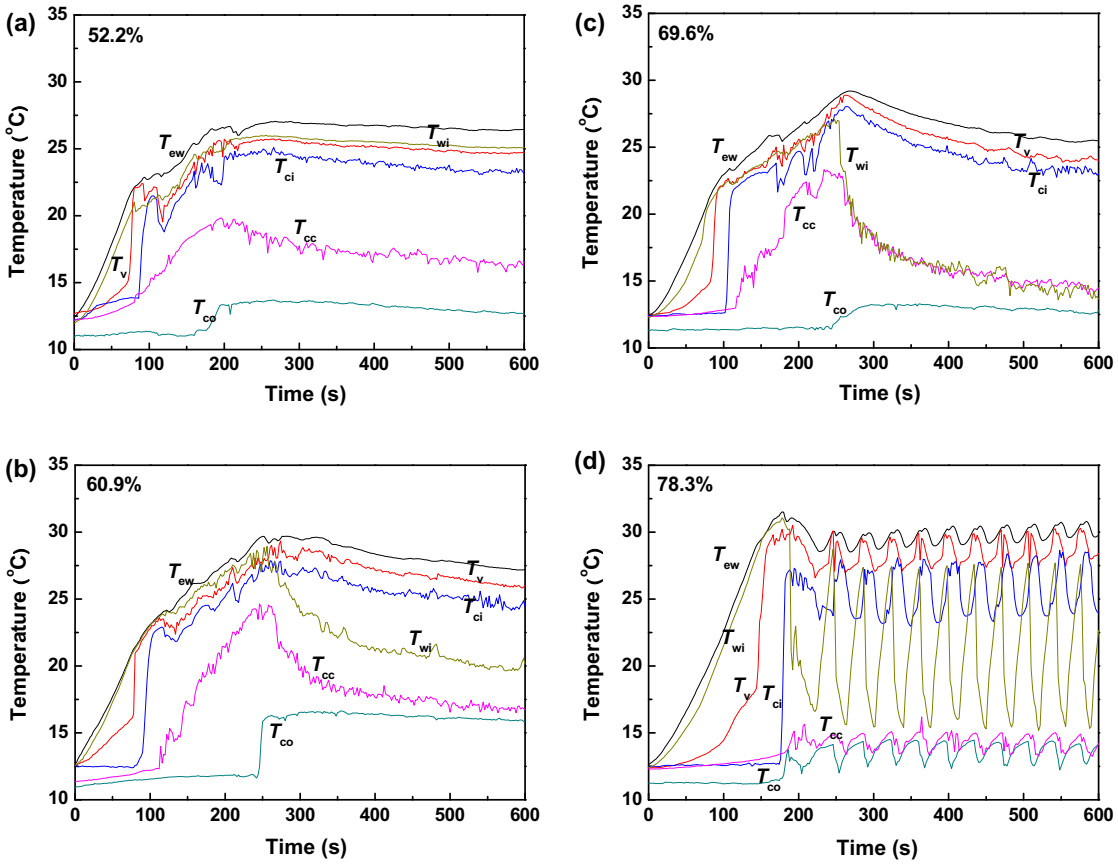

Fig. 2. Thermal response at the heat load of 30 W during the LHP start-up with different charge ratios.

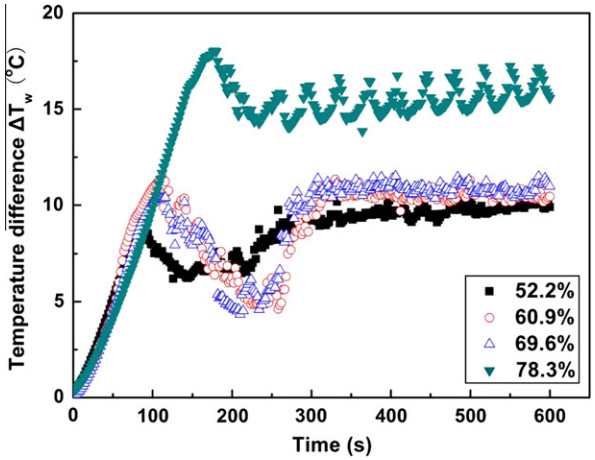

Fig. 3. Temperature differences during the LHP start-up with different charge ratios.

the start-up processes. A successful start-up can be identified by a sudden decrease of T_{cc} because the condensed fluid has entered the compensation chamber to cool the liquid in the chamber, and working fluid circulation is established.

The LHP that employed a 52.2% charge ratio started in 200 s and T_{ew} was maintained at approximately 26.5 °C, exceptionally fast for a start-up and low for an evaporator wall temperature, respectively. This performance was attributed to only 0.8 ml of water (23.2 ml for the combined evaporator and compensation chamber volume and 24 ml for the inventory) left in the vapor and liquid lines. Thus, a vapor–liquid interface was soon created in the evaporation zone, and the necessary pressure difference to displace the 0.8 ml of water to the compensation chamber in Eq. (1) was relatively small. Hence, water was easily displaced from the vapor–liquid line to the compensation chamber, and no temperature overshoot profile was observed during the start-up process. According to Eq. (1), creating a high value of dP/dT or high ΔT_w is not necessary due to the low required pressure difference. Hence, the evaporator wall temperature was only approximately 26.5 °C, and the temperature difference after the start-up was the lowest, as shown in Fig. 3.

As the inventories were increased to 60.9% and 69.6%, their respective temperature profiles remained quite the same, indicating an evident common temperature overshoot during the start-up process. The peak temperatures were 29.7 and 29.2 °C for the 60.9% and 69.6% inventories, respectively. The start-up duration took approximately 260 s, when T_{cc} began to decrease dramatically. After the circulation was established, all temperatures except T_{co} decreased and reached gradually a thermal stability condition. The wall temperature overshoots were 2.5 and 3.7 °C for the 60.9% and 69.6% inventories, respectively, which were the wall temperature differences between the peak and stable temperatures. Compared with the 52.2% inventory, the 60.9% and 69.6% inventories had more difficulty in starting the LHP. As much water was left in the vapor and liquid lines, the pressure difference required to drive the water was much larger than that of the 52.2% inventory. At the incipient start-up, the heat applied to the evaporator accumulated in the form of vapor in the evaporation zone and the vapor line and resulted in the increase in temperature. The vapor blocked in the evaporation zone produced high pressure. When the pressure difference was large enough, the vapor was driven into the condenser, and heat was dissipated efficiently. Subsequently, all temperatures except T_{co} began to decrease, and temperature overshoot was observed. The temperature difference (ΔT_w) and the saturation temperature of the LHPs with 60.9% and 69.6% inventories were slightly higher than those of the 52.2% inventory in the stable condition due to a relatively high fluid inventory.

For the LHP charged with 78.3% inventory, although the required pressure drop was large due to high inventory, the heat leak through the liquid-saturated wick was small. T_{cc} was much lower than the temperatures of the other charge ratios, and the temperature difference between T_{ew} and T_{cc} was large. Based on Eq. (1), building enough pressure drop did not take a long time, and the start-up time was not over 200 s, which was even faster than that of the 52.2% inventory. However, strong temperature oscillation was present throughout the process. The peak temperature was 31.5 °C, and T_{ew} fluctuated around 29 °C, with a maximum limit of ±1.5 °C after the successful start-up. The reason could be that the compensation chamber was filled with working fluid and allowed the subcooled fluid to be absorbed in the wick; thus, unstable vapor generation occurred, and overheating the working fluid took only a short period of time. During this period, T_{ew} and T_{wi} increased, whereas T_{ci} decreased under low vapor flow rate. These phenomena occurred periodically and resulted in strong temperature oscillation.

Fig. 3 shows that the temperature differences (ΔT_w) mainly underwent two increasing processes during the start-up. The first increasing process was determined by T_{ew} when the evaporator wall temperature increased as a result of the nucleate boiling activity during the incipient start-up. At the same time, the wick was saturated with liquid, and T_{cc} was low due to minor heat leak. The peak value of the difference between T_{ew} and T_{cc} roughly increased with the increase in the inventory, indicating that the amount of working fluid inventory was the main factor that determines superheat during the incipient start-up. When the vapor was driven into the condenser (an abrupt increase of T_{ci}), T_{ew} started to decrease, and T_{cc} began to increase, resulting from the increase in heat leak in the evaporation zone because the wick was no longer saturated with liquid. Therefore, the trend of ΔT_w changed from an increasing to a decreasing trend. To maintain sufficient ΔP_{ext}, the LHP saturation temperature also increased, which produced a high dP/dT value. This condition continued until the condensed liquid returned to the compensation chamber. When water entered the compensation chamber, circulation was established, and the fluid in the chamber cooled. Consequently, decline in T_{cc} was observed, and the second increasing process of ΔT_w is shown in Fig. 3. Simultaneously, T_{ew} also decreased because ΔT_w was large enough to create adequate ΔP_{ext}. No decrease in T_{ew} was observed in the case of the 52.2% inventory due to severe heat leak. Fig. 3 shows that the ΔT_w values also increased with the increase in inventory when start-up was completed. Considering the fact that the LHP with 78.3% charge ratio can start faster than the others, conclusion was made that the copper–water LHP with high inventory has a fast start-up process, although at the cost of temperature pulsation. In principle, however, LHP operation without temperature pulsation is impossible [3] because self-regulation of temperature and pressure is an intrinsic characteristic of LHPs.

Further, due to the low evaporator thermal resistance and high heat-exchange efficiency of the copper wick, the peak temperature did not rise to more than 32 °C, and the stable temperature remained at the 30 °C level. Starting the LHP successfully took no more than 260 s, exceedingly fast at such a low heat flux of 8.5×10^3 W/m^2.

3.2. LHP operating characteristics

The LHP operating characteristics, namely, evaporator wall temperature (T_{ew}), fluid temperature in the compensation chamber (T_{cc}), and evaporator core temperature (T_{wi}) versus heat load, under different charge ratios are shown in Fig. 4. As the ambient temperature (12 ± 0.5 °C) was only 2 °C higher than the sink

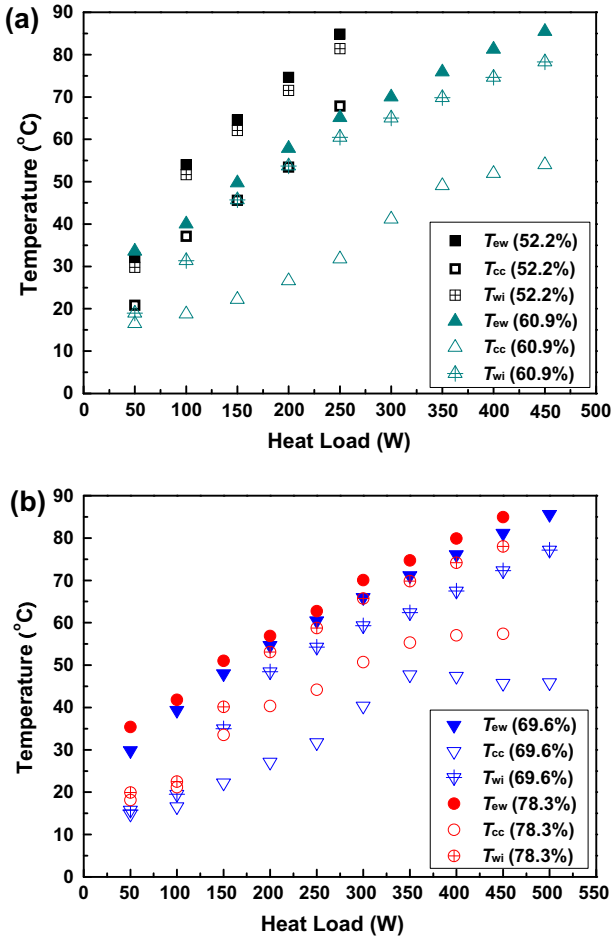

Fig. 4. LHP operating characteristics.

temperature (10 ± 0.5 °C), the T_{ew} curves increased linearly as the heat load increased, and the LHPs operated in a constant conductance mode throughout the tests. During the operation, the compensation chamber temperature (T_{cc}) was related to the evaporator wall temperature (T_{ew}), and the compensation chamber exchanged heat with the evaporator and the liquid that returned from the condenser [21]. In other words, the heat leak from the evaporator can be compensated by the subcooled liquid from the condenser in the compensation chamber; therefore, the T_{cc} value is the result of the energy balance between the evaporator and the condenser. As T_{wi} is attached to the internal surface of the wick, the temperature difference between T_{cc} and T_{wi} can be considered as a sign that identifies whether the heat leak is severe. If the wick is liquid-saturated, then the heat leak to the compensation chamber will be small, which can be recognized by a small temperature difference between T_{cc} and T_{wi}. When the heat load increases, the heat leak will dramatically increase and result in an abrupt increase of T_{wi}. However, owing to the subcooled liquid from the condenser, the increase of T_{cc} will not be as high as T_{wi}. Thus, a large temperature difference between T_{cc} and T_{wi} is observed.

The heat-transfer capacity of the LHP with 52.2% inventory under allowable evaporator wall temperature of 85 °C was only 250 W. Heat leak was severe throughout the test even when the heat load was only 30 W (start-up process). When the heat load increased to 50 W, although T_{cc} experienced an evident decline, T_{wi} still maintained a high temperature of approximately 1.5 °C lower than T_{ew}, as shown in Fig. 4a. As the heat load increased, T_{cc} failed to maintain a low value, resulting in a high evaporator wall temperature. Reasonable assumption can be made that the 52.2% charge ratio (fluid inventory: 24 ml) is low for the copper–water LHP to solve the heat-leak problem, especially for low thermal resistance evaporator. This concept was also verified by the fluid inventory calculated between the cold and hot cases (26.8–37.7 ml).

When the charge ratios were increased, the maximum heat-transfer capacities reached up to 450 and 500 W for 60.9% and 69.6% charge ratios, respectively. From the temperature readings of T_{cc} and T_{wi}, higher inventories ensured that heat leak was suppressed under low heat-load range. Under heat loads of 50 and 100 W for the 60.9% and 69.6% charge ratios, respectively, the heat leak was small. As the heat load increased, T_{wi} increased abruptly, whereas T_{cc} also increased, which resulted in a large temperature difference between T_{cc} and T_{wi}, indicating that heat leak dramatically increased. When the heat load increased to a high range (350 W and above), the slope of increasing T_{cc} became smaller owing to the high rate flow of the subcooled fluid from the condenser. Even T_{cc} started to decline in the case of the 69.6% charge ratio, and the temperature difference between T_{ew} and T_{wi} increased, showing an alleviation of heat leak. As the fluid inventory increased, available space for the vapor phase decreased and so did the amount of heat leak [11]. Although the heat leak that occurred in LHPs with 60.9% and 69.6% charge ratios was also evident, T_{cc} still remained at a relatively low value to control the evaporator temperature and demonstrated a relatively high heat-transfer capacity because of high inventory.

The temperature curve of the 78.3% inventory was similar to that of the 69.6% inventory. Under a low heat-load range (50–100 W), the heat leak was minor. Thereafter, the heat leak increased significantly with the increase in the heat load. In addition, the slope of increasing T_{cc} became smaller owing to the high flow rate of subcooled fluid from the condenser when the heat load increased to a high range (350 W and above). However, T_{ew} of the 78.3% inventory was approximately 3 °C higher than that of the 69.6% inventory under the same heat load because of its high start-up temperature. Further, T_{cc} of the 78.3% inventory was consistently higher than that of the 69.6% inventory throughout the test, as shown in Fig. 4b. Thus, a heat transfer capacity of 450 W was attained.

Higher inventory is indeed an effective method for copper–water LHP to alleviate heat leak. In low heat-load range, a saturated wick is assured with more working fluid inventory, whereas high working fluid flow rate from the condenser will control the fluid temperature in the compensation chamber in the high heat-load range. Thus, the maximum heat-transfer capacity of the 69.6% inventory was up to 500 W, and 450 W was also achieved for the 60.9% and 78.3% inventories. Despite the side effect of extremely high inventory observed in the case of the 78.3% charge ratio, copper–water LHP with high inventories (60.9%–78.3%) have a high heat-transfer capacity during the LHP operations.

3.3. Thermal resistance

The evaporator and LHP thermal resistances with four inventories are shown in Figs. 5 and 6, respectively. According to Chernysheva [22], three vapor–liquid distributions, namely, a saturated wick, a two-phase layer in the wick, and a dry zone near the wall, are present one after the other with the increase in the heat load, which can be determined from the evaporator thermal resistance. The evaporator thermal resistance is composed of the evaporator wall thermal resistance R_{wall}, contact thermal resistance R_{cont}, and wick thermal resistance R_w. The contribution of the first two thermal resistances in the total evaporator thermal resistance can be considered as constant, whereas wick thermal resistance R_w is determined by the wick saturation condition and the location of the evaporating menisci. Fig. 5 shows that the evap-

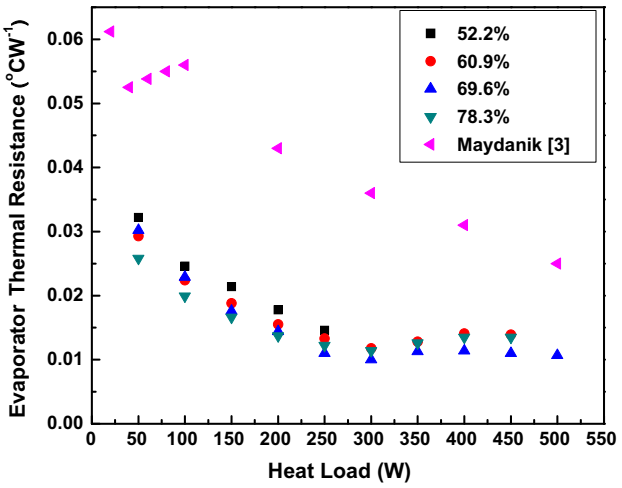

Fig. 5. Evaporator thermal resistance.

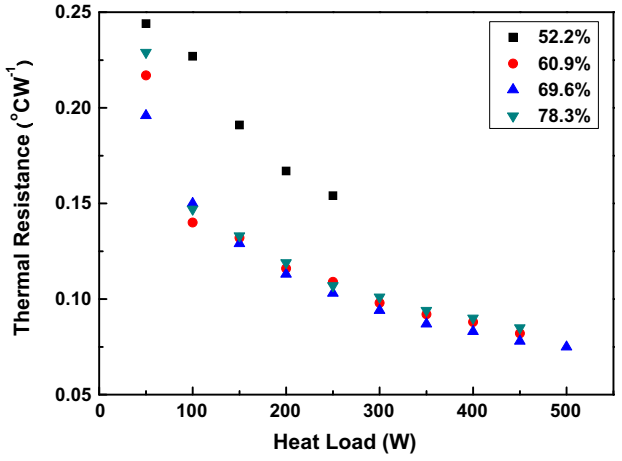

Fig. 6. LHP thermal resistance.

orator thermal resistance from Maydanik et al. [3] is much higher than the present LHP under the heat load range from 20 to 500 W, attributed to the low contact thermal resistance that results from the metallurgical bonding between the envelope and the wick surface. The 52.2% inventory values were clearly higher than any of the others due to the presence of the dry zone in the wick throughout the test as a result of low inventory. The values of the other inventories decreased as the heat load increased and attained minimum values under the heat load of 300 W. The minimum value of the evaporator thermal resistance resulted from the presence of a two-phase evaporating layer in the wick, believed to be the most effective evaporation mode [20]. Subsequently, all values began to increase because a dry-wick zone started to occur near the evaporator wall, and the thermal resistance of the dry zone R_{dry} was introduced to wick thermal resistance R_w, resulting in a higher evaporator thermal resistance. The minimum evaporator thermal resistance was only 0.010 °C/W under 300 W for the LHP with the optimum 69.6% inventory.

The LHP thermal resistances of the 52.2% inventory, which ranged from 0.15 °C/W to 0.24 °C/W, were the highest throughout the test because severe heat leak caused high saturation temperature and resulted in high evaporator wall temperature. The thermal resistances of the 78.3% inventory were a little higher than those of the 60.9% and 69.6% inventories. The minimum thermal resistance of the test was only 0.075 °C/W under 500 W for the LHP with 69.6% inventory. These values were relatively low due to the low thermal resistance that resulted from the new connection design.

4. Conclusion

In this paper, copper–water LHPs with charged ratios that ranged from 52.2% to 78.3% have been fabricated to investigate the effect of inventory on heat-transfer performances, including start-up and heat-transfer capacity. Based on the experimental results, the following conclusions were drawn:

(1) Copper–water LHPs with different inventories started smoothly in not more than 260 s under a heat load of 30 W (heat flux of 8.5×10^3 W/m^2), and a high heat-transfer capacity was attained under allowable evaporator wall temperature of 85 °C: 500 W for the 69.6% inventory and 450 W for the 60.9% and 78.3% inventories. Hence, the proposed LHP with copper–water combination can start fast and attain high heat-transfer capacity in the temperature range below 100 °C.

(2) The chance of vapor leakage was eliminated owing to the new evaporator design. A low evaporator thermal resistance of 0.010 °C/W under 300 W for the LHP with a 69.6% charge ratio was also achieved, which contributed to an efficient heat exchange in the evaporation zone and a relatively low thermal resistance of 0.075 °C/W under 500 W for the LHP with a 69.6% charge ratio.

(3) Based on the parameters mentioned above, high inventory is an effective method for suppressing heat leak. The liquid-saturated wick in low heat-load range is guaranteed to improve the start-up owing to high inventory, and high subcooled liquid flow rate from the condenser can be realized to cool the fluid in the compensation chamber under medium and high heat-load range. However, side effects of the extremely high inventory (78.3%), such as a strong temperature oscillation during start-up and more heat leak during operation, were also observed in the research. Hence, the optimal inventory for the proposed LHP is about 70%, especially for the LHP with a high volume ratio (>50%) of the evaporator and the compensation chamber to the whole apparatus.

Acknowledgements

The authors are grateful for the support of the Shanghai "Phosphor" Science Foundation under Grant No. 11QA1401800.

References

[1] Y. Maydanik, Loop heat pipes, Applied Thermal Engineering 25 (2005) 635–657.
[2] C.C. Yeh, C.N. Chen, Y.M. Chen, Heat transfer analysis of a loop heat pipe with biporous wicks, International Journal of Heat and Mass Transfer 52 (2009) 4426–4434.
[3] Y. Maydanik, S. Vershinin, M. Chernysheva, S. Yushakova, Investigation of a compact copper–water loop heat pipe with a flat evaporator, Applied Thermal Engineering 31 (2011) 3533–3541.
[4] R. Singh, A. Akbarzadeh, M. Mochizuki, Operational characteristics of the miniature loop heat pipe with non-condensable gases, International Journal of Heat and Mass Transfer 53 (2010) 3471–3482.
[5] T. Kobayashi, T. Ogushi, S. Haga, E. Ozaki, M. Fujii, Heat transfer performance of a flexible looped heat pipe using R 134a as a working fluid: Proposal for a method to predict the maximum heat transfer rate of FLHP, Heat Transfer Asian Research 32 (4) (2003) 306–318.
[6] J.H. Boo, W.B. Chung, Thermal performance of a loop heat pipe having propylene wick in a flat evaporator, in: Proceedings of the ASME Heat Transfer Conference, San Francisco, CA, 2005.
[7] P.H.D. Santos, E. Bazzo, S. Becher, R. Kulenovic, R. Mertz, Development of LHPs with ceramic wick, Applied Thermal Engineering 30 (2010) 1784–1789.

[8] P.H.D. Santos, E. Bazzo, A.A.M. Oliveira, Thermal performance and capillary limit of a ceramic wick applied to LHP and CPL, Applied Thermal Engineering 41 (2012) 92–103.
[9] H. Li, Z.C. Liu, B.B. Chen, W. Liu, C. Li, J.G. Yang, Development of biporous wicks for flat-plate loop heat pipe, Experimental Thermal and Fluid Science 37 (2012) 91–97.
[10] J. Xu, Y. Zou, M. Fan, L. Cheng, Effect of pore parameters on thermal conductivity of sintered LHP wicks, International Journal of Heat and Mass Transfer 55 (2012) 2702–2706.
[11] W. Joung, T. Yu, J. Lee, Experimental study on the loop heat pipe with a planar bifacial wick structure, International Journal of Heat and Mass Transfer 51 (2008) 1573–1581.
[12] G.P. Celata, M. Cumo, M. Furrer, Experimental tests of a stainless steel loop heat pipe with flat evaporator, Experimental Thermal and Fluid Science 34 (2010) 866–878.
[13] L. Vasiliev, D. Lossouarn, C. Romestant, A. Alexandre, Y. Bertin, Y. Piatsiushyk, V. Romanenkov, Loop heat pipe for cooling of high-power electronic components, International Journal of Heat and Mass Transfer 52 (2009) 301–308.
[14] G. Xin, K. Cui, Y. Zou, L. Cheng, Reduction of effective thermal conductivity for sintered LHP wicks, International Journal of Heat and Mass Transfer 53 (2010) 2932–2934.
[15] R. Singh, A. Akbarzadeh, M. Mochizuki, Effect of wick characteristics on the thermal performance of the miniature loop heat pipe, Journal of Heat Transfer ASME 131 (2009) 082601-1–080601-10.
[16] S.F. Wang, W.B. Zhang, X.F. Zhang, J.J. Chen, Study on start-up characteristics of loop heat pipe under low-power, International Journal of Heat and Mass Transfer 54 (2011) 1002–1007.
[17] J.H. Boo, W.B. Chung, Thermal performance of a small-scale loop heat pipe with PP wick, in: 13th IHPC, Shanghai, China, 21–25 September, 2004, pp. 259–264.
[18] J. Xu, L. Zhang, H. Xu, Performance of LHPs with a novel design evaporator, International Journal of Heat and Mass Transfer 55 (2012) 7005–7014.
[19] S. Launay, V. Sartre, J. Bonjour, Parametric analysis of loop heat pipe operation: a literature review, International Journal of Thermal Science 46 (2007) 621–636.
[20] S.J. Kline, F.A. McClintock, Describing uncertainties in single-sample experiments, Mechanical Engineering 75 (1953) 3–8.
[21] K. Jentung, Operating characteristics of loop heat pipes, in: 29th International Conference on Environmental System, Colorado, USA, 1999.
[22] M. Chernysheva, Y. Maydanik, Heat and mass transfer in evaporator of loop heat pipe, Journal of Thermo Physics and Heat Transfer 23 (2009) 725–731.